Check for updates

Super protective anti-bacterial coating development with silica–titania nano core–shells

Jaya Verma, [ID] *[a] A. S. Khanna,[b] Rachana Sahney[c] and Arpita Bhattacharya[a]

In the present study, we have developed an anti-bacterial as well as mechanically-strengthened super protective coating material, which can be used as a marine antifouling paint. In this research, silica, titania and silica–titania core–shell nanoparticles were individually prepared *via* sol–gel and peptization processes. The idea behind the synthesis of core–shell nanoparticles was to utilize the mechanical strength of silica and the antimicrobial property of TiO_2 together. These nanoparticles were characterized *via* dynamic light scattering, UV-Visible spectroscopy, X-ray diffraction, scanning electron microscopy, energy-dispersive X-ray spectroscopy, transmission electron microscopy and X-ray photoelectron spectroscopy. Coating formulations were developed with two types of model binders, *i.e.*, solvent-based polyurethane and water-based poly-acrylic, containing all nanoparticles individually at various concentrations for a better comparative study. These coating formulations were applied onto mild steel for anti-bacterial testing that was performed against *Escherichia coli* and *Bacillus*. The nanoparticle concentration was varied from 1% (wt) to 6% (wt). The best anti-bacterial result was obtained with 4% (wt) of silica–titania core–shell nanoparticles prepared *via* the peptization process among all the nanoparticles. The scratch testing was performed successfully using an Erichsen scratch tester; the formulated PU coating passed up-to 20 N load with good adhesion, impact resistance, flexibility and has shown satisfactory anti-corrosion performance.

1. Introduction

Paint is a synthetic substance commonly used to provide texture to infrastructure, furniture and utensils in everyday life. The deterioration of paint on surfaces or in the environment causes its components to be mineralized. This corrosion on the surface is not only an economic loss but also results in the release of harmful degradation products into the environment causing an alarming situation. Although there are certain chemical approaches available for the removal of degraded products, these methods have some disadvantages.[1]

Microorganisms are also renowned for their potential to degrade synthetic compounds, and various microbial species are reported for paint degradation. Major groups of microbes, involved in paint degradation are bacteria and fungi.[2,3] In this study, we used two types of bacteria, Gram-negative and Gram-positive, *i.e.*, *E. coli* and *Bacillus*, respectively.

E. coli is in the bacterial domain of single-celled prokaryotes (Fig. 1a). *E. coli* can cause food poisoning, breathing problems, diarrhea, abdominal pain, dehydration, urinary tract infections

and kidney failure.[4–7] The water swallowed during swimming in a pool, lake, or pond contains *E. coli*, which causes 75% to 95% of urinary tract infections.[8,9] The other one, *Bacillus* is aerobic or anaerobic bacteria widely found in soil and water (Fig. 1b). *Bacillus* species frequently occur in chains and cause skin infection.[10,11] As such, antibacterial coatings are needed for defined surfaces.

This type of coating can be useful as an *antifouling coating* for the marine industry, wherein it would be applied to the underwater hull of ships, discouraging or preventing the growth of organisms that attach to the hull. It also improves the flow of water passing through the hull of a fishing vessel or high-performance racing yacht because of the smoothness of the coatings.

In previous studies, numerous researchers have worked on the antibacterial effects of nanoparticles using nanoparticles, such as TiO_2 and ZnO, but no one has worked on silica–titania core–shell nanoparticles for antibacterial paint applications.

2. Experimental-materials and methods

In this study, we formulated silica,[12–15] titania,[16–19] and silica–titania[20–22] core–shell nanoparticles individually *via* sol–gel and peptization processes.[23] In a core–shell structure, silica (core material) improves the strength of the coating[24,25] and a thin layer of titania on silica improves the antibacterial property in a single

[a]Amity Institute of Nanotechnology, Amity University, Noida, Uttar Pradesh-201303, India. E-mail: jayaverma123@yahoo.com

[b]Surface Engineering & Coating Consultant, Mumbai-400078, India

[c]Amity Institute of Biotechnology, Amity University, Noida, Uttar Pradesh-201303, India
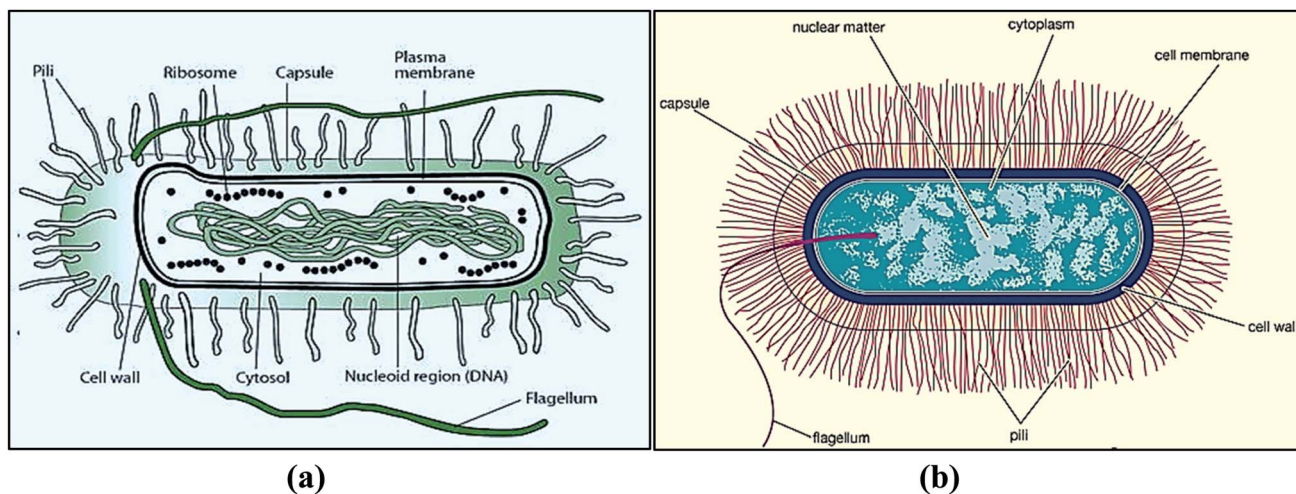
Fig. 1 Structure of bacteria (a) *E. coli* and (b) *Bacillus* [source: www.britannica.com].

material.[26] Titania has substantial advantages over both chemical and metal-based systems. First, titania nanoparticles have a broad spectrum of activity against microorganisms, including Gram-negative and Gram-positive bacteria, and fungi, which is of particular importance for multiple drug-resistant strains.[27,28] Second, and more importantly, titania–polymer nano-composites are intrinsically environmentally friendly and exert a non-contact biocidal action. Therefore, no release of potentially toxic nano-particles (with unpredictable effects on human health) into the media is required to achieve disinfection capabilities.[29,30] Anatase TiO$_2$ coating has been formulated in this study. This form of TiO$_2$ is highly crystalline in nature because of the large bandgap ∼3.2 eV and shows better antibacterial activity as compared to rutile TiO$_2$ (bad gap = ∼3.0 eV), as shown in Fig. 2.

This core–shell formulation also became cost-effective as compared to pure titania coatings and improved the properties of two different materials in a single nanoparticle. These coatings were developed in solvent-based and water-based emulsion, *i.e.*, polyurethane and poly-acrylic.[31,32]

2.1. Materials

Nutrient broth was purchased from HiMedia Laboratories Pvt Limited (India). Poly-acrylic and polyurethane were purchased from Dalton Chemicals Pvt Limited (India). Ethanol was bought from Merck (India) and ammonium hydroxide from Qualikems Fine Chemical Pvt. Ltd. (India). Titanium tetraisopropoxide (TTIP), tetraethyl orthosilicate (TEOS) and methyl trimethoxy-silane (MTMS) were purchased from Sigma Aldrich Chemicals Pvt Limited (India).

2.1.1 Instruments. UV-Visible double beam spectropho-tometer (Shimadzu UV-1800), Malvern Instruments-Zetasizer Nano S-90, Bruker D8 Focus X-ray diffractometer, FEI Tecnai G2 F20-S TWIN TEM and XPS Zeiss-Neon 40, Erichsen scratch tester were used.

2.2. Methods

2.2.1 Preparation of silica, titania and silica–titania core–shell nanoparticles. Core silica was prepared using tetraethyl orthosilicate (TEOS) as a precursor in the presence of H$_2$O, C$_2$H$_5$OH and NH$_4$OH. Shell titania was developed on the core material using titanium tetraisopropoxide (TTIP) as a precursor in the presence of isopropyl alcohol and water mixture. The detailed synthesis procedure *via* both the processes, *i.e.*, sol–gel and peptization (Fig. 3), for the same nanoparticles is already reported in our previously published research articles (ref. 31 and 32).
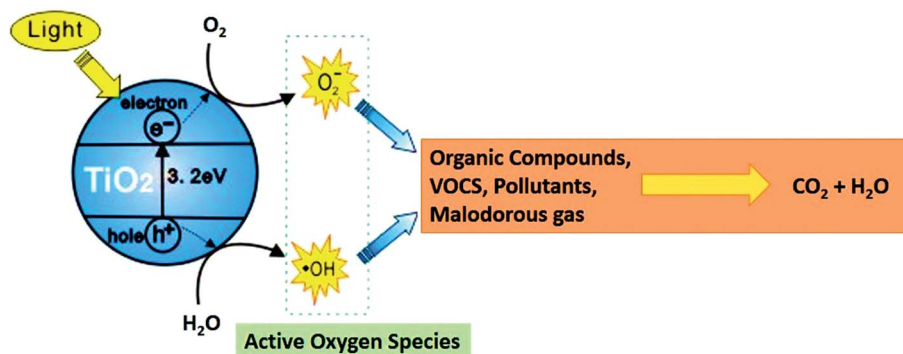

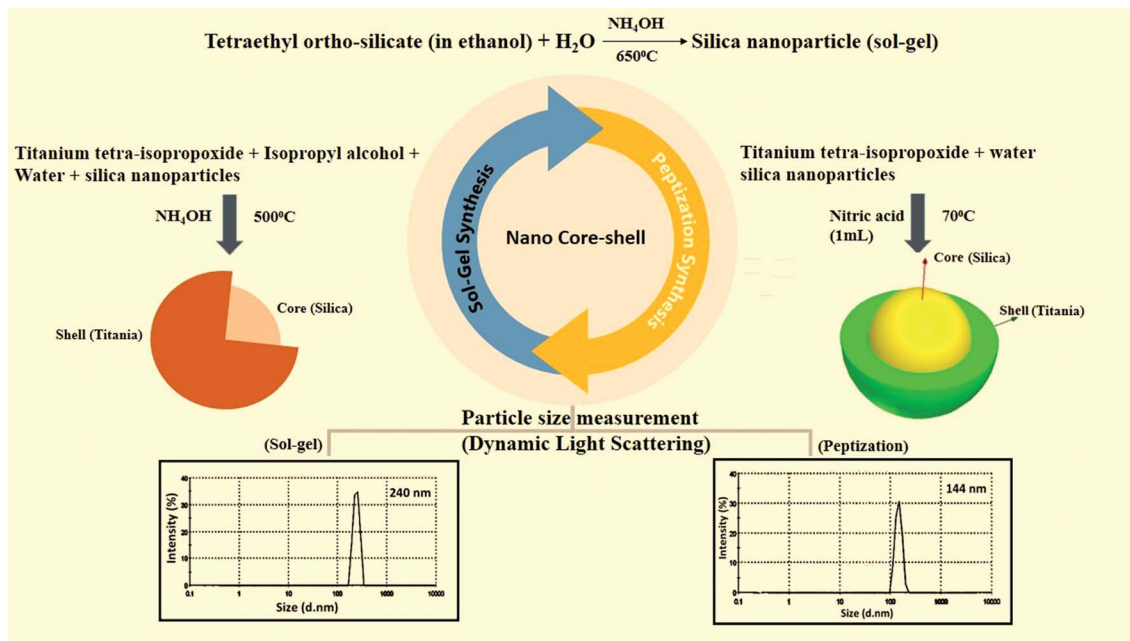**Fig. 2** Antimicrobial activity of TiO$_2$ nanoparticles.

Fig. 3   Synthesis of silica–titania core–shell nanoparticles.

2.2.2   Surface modification of the core–shell nanoparticles. The surface modification of silica–titania core–shell nano-particles was mainly carried out for better dispersion in solvent-based binder polyurethane and to get a smooth surface. In this study, methyl trimethoxy-silane (MTMS) was used for the surface modification of silica–titania core–shell nanoparticles. For the surface modification of the core–shell nanoparticles, 1 g of silica–titania core–shell particles were dispersed in 20 ml of ethanol. To this dispersion, 0.2 mL MTMS was added under

stirring conditions. After 4 h of stirring, 1 mL of ammonium hydroxide was added to this solution dropwise, and stirring was continued for another 1 h. Then, the obtained precipitate dried at 70 °C for 20–30 min so that ethanol could be removed and the functionalized core–shell nanoparticles were obtained.

2.2.3   Coating formulations. Poly-acrylic and polyurethane coatings were developed on mild steel containing silica, titania and silica–titania core–shell nanoparticles individually prepared *via* both the processes, *i.e.*, sol–gel and peptization, for
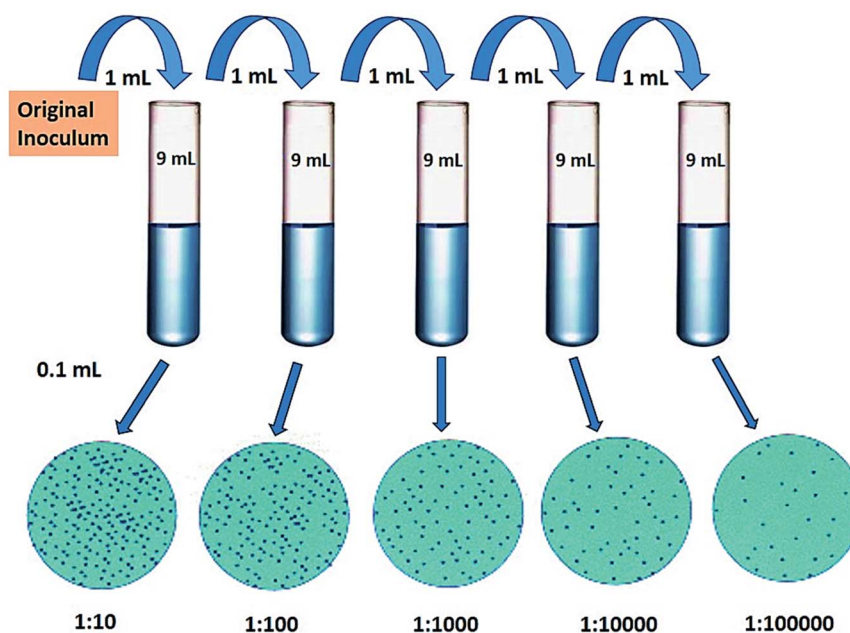

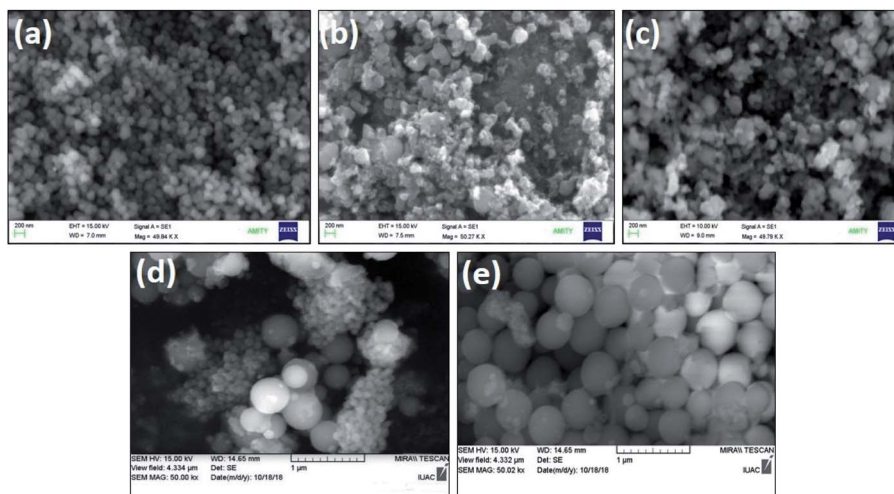Fig. 4   Serial dilution of a bacterial suspension of *E. coli*.

Fig. 5   SEM images of (a) silica nanoparticles (b) titania nanoparticles prepared through the sol–gel process (c) silica–titania core–shell nanoparticles prepared through the sol–gel process (d) titania nanoparticles prepared through the peptization process (e) silica–titania core–shell nanoparticles prepared through the peptization process.

antibacterial testing as well as mechanical property testing. The coating on a mild steel substrate was developed using a spray gun with a thickness of 30–40 μm. The nanoparticle concentration was varied from 1% (wt) to 6% (wt) in coating formulations.

3. Characterization and testing

The characterization of all the nanoparticles such as dynamic light scattering (DLS), UV-Vis spectroscopy, XRD analysis, and Fourier transform infrared spectroscopy was successfully performed. In this study, DLS was used to measure the particle size of the as-prepared nanomaterials. The particle size of nano-silica was measured as 85 nm. Nano-TiO_2 was measured as 107 nm, and the size of the silica–titania core–shell nanoparticles was 240 nm, prepared via a sol–gel process. TiO_2 nanoparticles and SiO_2–TiO_2 nano core–shell particles were also prepared by the peptization process with the particle size of 75 nm and 144 nm separately (Fig. 3). All these characterizations of the same nanoparticles are briefly described in our previously published research (ref. 31). Further studies on antibacterial and mechanical testing are discussed in this study. Optical density was measured for the bacterial growth. The analysis of coatings was performed on a UV-Visible double beam spectrophotometer (Shimadzu UV-1800), FEI Tecnai G2 F20-S TWIN TEM was used for TEM imaging, a Zeiss scanning electron microscope was used for the SEM analysis. The confirmation of the silica–titania core–shell nanoparticle formation was performed via X-ray photoelectron spectroscopy (XPS Zeiss-Neon 40) and an Erichsen scratch tester was used for the anti-scratch testing analysis.
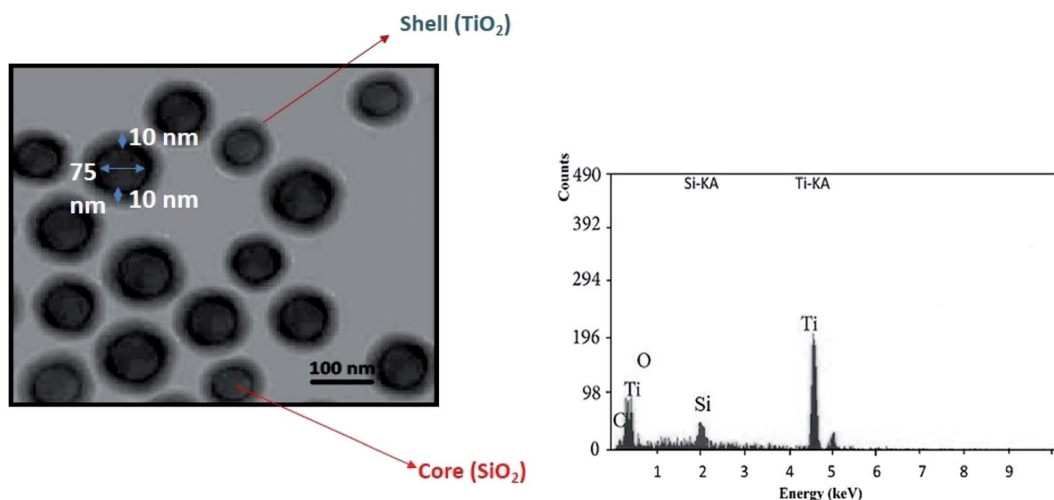

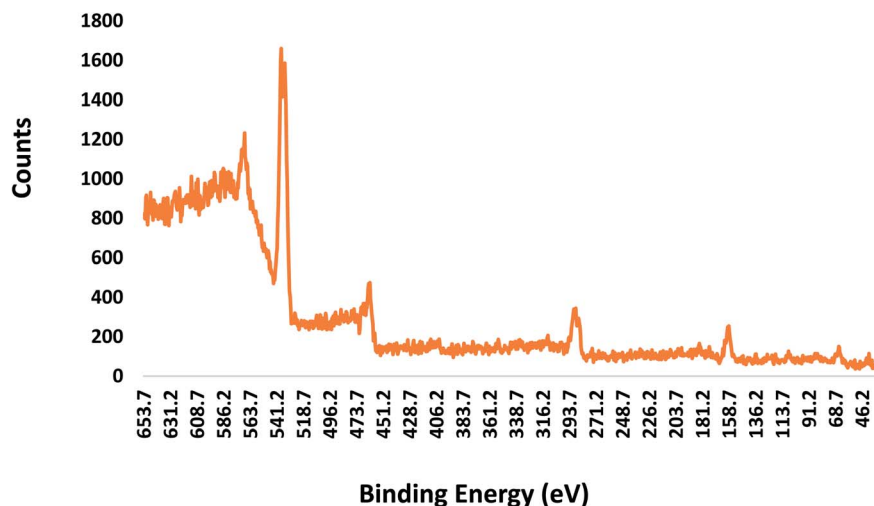Fig. 6   TEM and EDX analysis of silica–titania core–shell nanoparticles.

Fig. 7 XPS of silica–titania core–shell nanoparticles.

Table 1 Optical density data of bacterial culture media containing nanoparticles with *E. coli* at 24 h

Material (nanoparticles)	Optical density at 600 nm
Control	0.9
SiO_2 nanoparticles	0.3
TiO_2 (sol–gel) nanoparticles	0.2
TiO_2 (peptization) nanoparticles	0.11
Silica–titania core–shell (sol–gel) nanoparticles	0.19
Silica–titania core–shell (peptization) nanoparticles	0.09

3.1 Anti-bacterial testing

The antibacterial activity of core–shell nanocomposites was investigated qualitatively and quantitatively. Anti-bacterial testing was performed by dissolving 7.5 g of nutrient broth in 500 mL of distilled water under stirring. This solution was sterilized by autoclaving at 121 °C at 15 psi for 30 min and was cooled to room temperature. Then, this media was divided into several parts; 20 mL in each test-tube. Free particles and coated mild steel were added in separate test-tubes in the presence of bacteria *E. coli* and *Bacillus*. The nanoparticle content was varied from 1% (wt) to 6% (wt) in the media and in the coating form also. After this, test tubes were placed on a shaker for 24 h and optical density was measured at 600 nm and 6 h interval upto 24 h of these samples.

The quantitative examination of the bacterial activity for *E. coli* and *Bacillus* was estimated by the survival ratio as calculated from the number of viable cells, which form colonies on the nutrient agar plates. The colony forming units (CFU) were calculated for these samples by growing bacteria in Petri-plates. The serial dilutions of bacterial cultures were prepared from 1 : 10, 1 : 100, 1 : 1000,
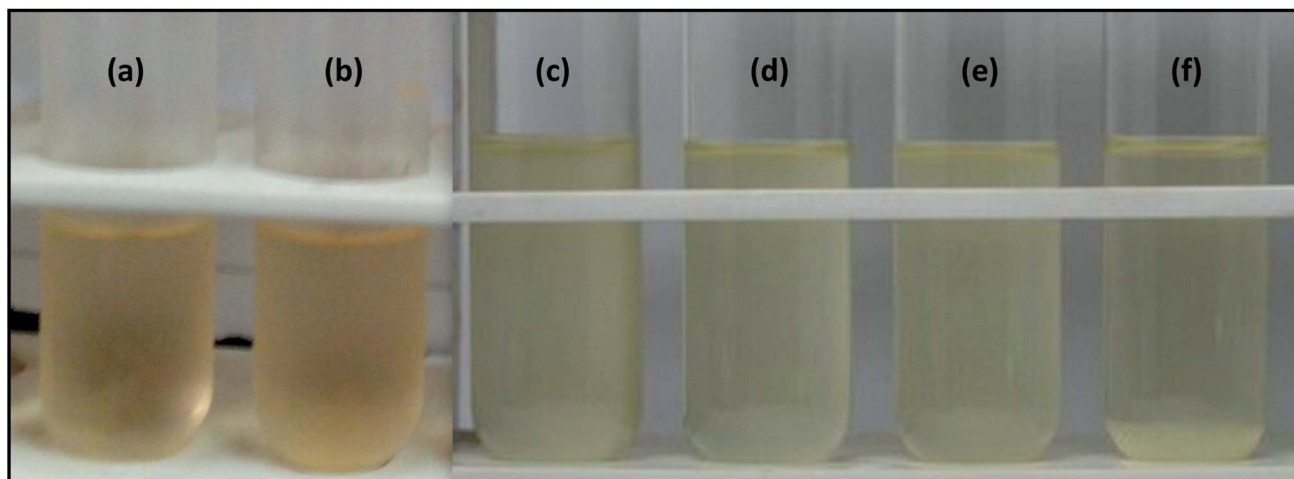

Fig. 8 Anti-bacterial testing of nanoparticles against *E. coli* (a) control (b) silica nanoparticles (c) titania nanoparticles prepared through the sol–gel process (d) titania nanoparticles prepared through the peptization process (e) silica–titania core–shell nanoparticles prepared through the sol–gel process (f) silica–titania core–shell nanoparticles prepared through the peptization process.
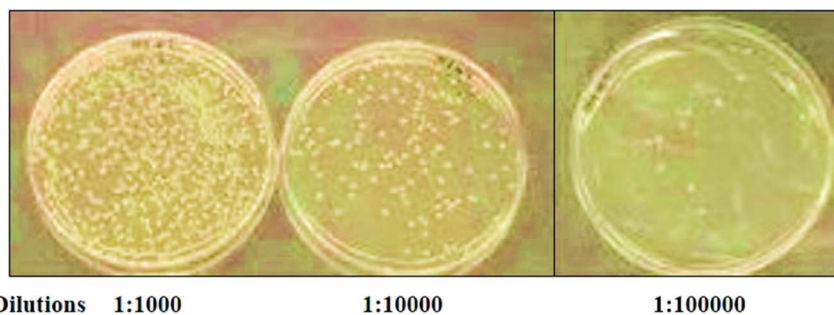
Fig. 9 Colonies formed after serial dilutions of *E. coli* bacterial culture.

Table 2 Optical density data of bacterial culture media containing PA-based nanocoatings with *E. coli* at 24 h

Material (Coatings)	Optical density at 600 nm
Control	0.9
Only substrate	0.85
Pure poly-acrylic (PA) coating	0.4
PA/SiO$_2$ nano-coating	0.29
PA/TiO$_2$ (sol–gel) nano-coating	0.17
PA/TiO$_2$ (peptization) nano-coating	0.08
PA/silica–titania core–shell (sol–gel) nano-coating	0.14
PA/silica–titania core–shell (peptization) nano-coating	0.06

Table 3 Optical density data of bacterial culture media containing PU-based nanocoatings with *E. coli* at 24 h

Material	Optical density at 600 nm
Control	0.9
Only substrate	0.85
Pure polyurethane (PU) coating	0.45
PU/SiO$_2$ nano-coating	0.24
PU/TiO$_2$ (sol–gel) nano-coating	0.1
PU/TiO$_2$ (peptization) nano-coating	0.03
PU/silica–titania core–shell (sol–gel) nano-coating	0.08
PU/silica–titania core–shell (peptization) nano-coating	0.00

Table 4 Optical density data of bacterial culture media nanoparticles with *Bacillus* at 24 h

Material (nanoparticles)	Optical density at 600 nm
Control	0.99
SiO$_2$ nanoparticles	0.71
TiO$_2$ (sol–gel) nanoparticles	0.55
TiO$_2$ (peptization) nanoparticles	0.38
Silica–titania core–shell (sol–gel) nanoparticles	0.45
Silica–titania core–shell (peptization) nanoparticles	0.29

1 : 10 000 and 1 : 1 00 000. A final dilution (0.5 OD), 0.1 mL of culture was used as a standard bacterial culture for CFU (Fig. 4). At this dilution, all the as-prepared nanoparticles and nano-coatings were added to count the colonies formed in Petri plates.

3.2 Mechanical testing

Using the Erichsen scratch tester, anti-scratch testing was performed up to 20 N load on a mild steel panel. The coating was developed on a 2×4 inch mild steel panel *via* the spray gun and dried at 100 °C for 15 min. This spray coating thickness measured was 30–40 μm. Few other mechanical properties were also analyzed on this coating such as the adhesion test using a cross-hatch tester. Impact resistance was checked by applying a certain load at a certain distance of this PU-based coatings. The flexibility of these coating films was also measured.

3.3 High humidity testing

The anti-corrosion performance of the coating was analyzed by high humidity testing. In this method, a sealed chamber was used in which we maintained the required atmosphere for the testing, and the temperature was 100 °F and humidity levels were near 97%. Test specimens are left in the chamber for a full 24 h and we found that samples passing this test exhibit no signs of rust or staining at the surface.

4. Results and discussion

4.1 Analysis on the surface morphology of the nanoparticles using a scanning electron microscope

The scanning electron microscopy study was successfully carried out on silica, titania and silica–titania core–shell nanoparticles, as shown in Fig. 5. The formation of core–shell nanoparticles is shown in Fig. 5(c) and (e) with individual silica [Fig. 5(a)] and titania [Fig. 5(b) and (d)] nanoparticles. Silica nanoparticles were spherical and smooth, whereas titania and core–shell nanoparticles were faceted in structure when prepared *via* a sol–gel process. Titania and core–shell nanoparticle prepared *via* the peptization process are found to be spherical in shape.

4.2 Transmission electron microscopy and energy dispersive X-ray spectroscopy of silica–titania core–shell nanoparticles

TEM (transmission electron microscopy) was performed on prepared core–shell nanoparticles to confirm the formation
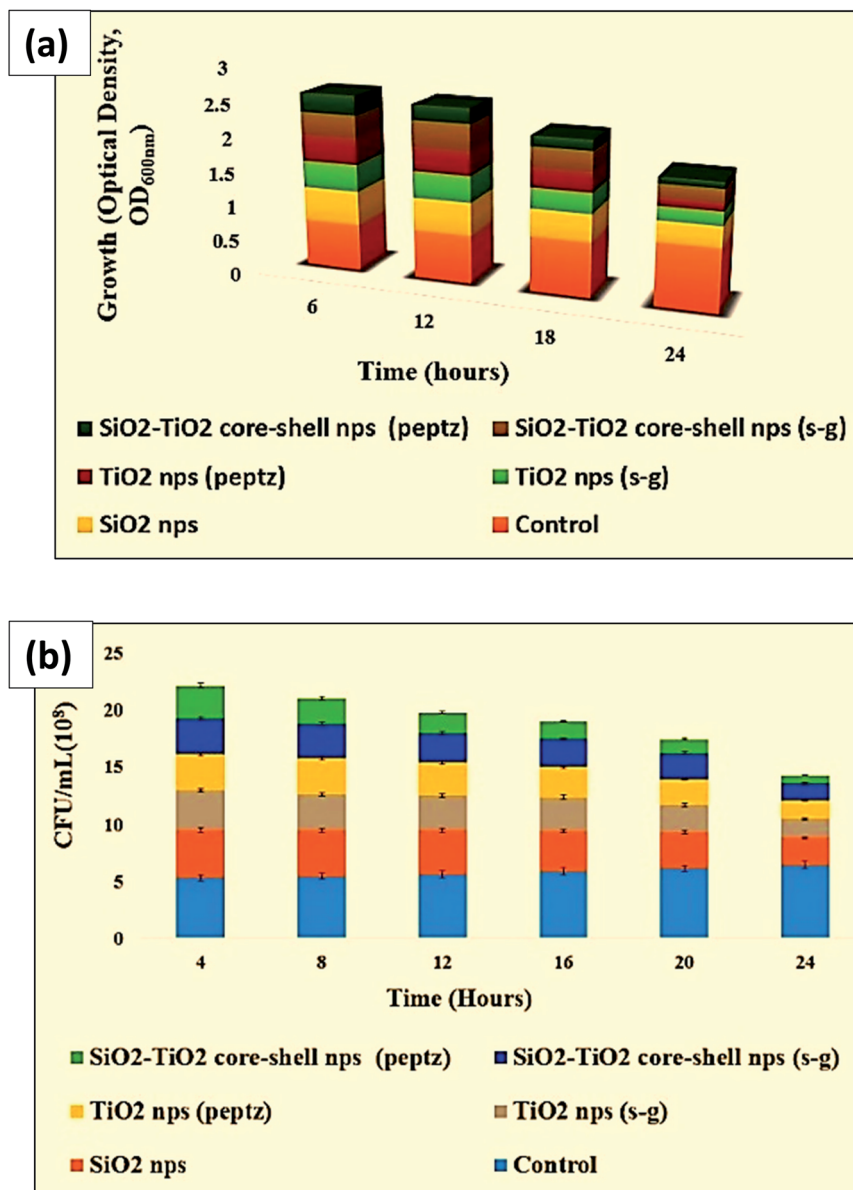
Fig. 10   (a) Optical density and (b) CFU of all prepared nanoparticles in antibacterial testing against *E. coli*.

of a core–shell structure with a particle size of around 100 nm in spherical shape, as shown in Fig. 6. This analysis was performed at 20 kV and 100× magnification with a point resolution of 0.25 nm. TEM revealed the primary particle size of the core–shell nanoparticle. The previous measurements of the particle size *via* DLS was carried out to determine the true state of the particle in media, *i.e.*, around 144 nm. The difference in the size of the core–shell particle was because the measurement was carried out in the liquid state and as the solvent molecules associate with the particles, a larger size of the particle is seen when compared with the TEM analysis. The energy dispersive X-ray spectroscopy analysis was carried out to confirm the elemental composition of the material. The EDX and TEM analyses of the core–shell nanoparticles confirm the presence of silica in the core by its

low count rate and titania on the surface by its high-count rate.

4.3 X-ray photoelectron spectroscopy (XPS) analysis of silica–titania core–shell nanoparticles

Fig. 7 shows the XPS spectra of the core–shell nanoparticles. A few apparent peaks located at the binding energies of 285.4, 459.4, 465.2, 530.8, and 532.2 eV can be observed. The peak at the binding energy of 285.4 eV is assigned to the C 1s peak. The two peaks located at the binding energies of 459.4 and 465.2 eV correspond to the Ti 2p peak. The peaks for the pure Ti element are expected to appear at 455 (Ti 2p3/2) and 461 (Ti 2p1/2) eV. There were shifts in the Ti 2p3/2 and Ti 2p1/2 peak positions due to the presence of tetravalent Ti (Ti^{4+}), as expected in TiO_2. On the other hand, the peaks at the
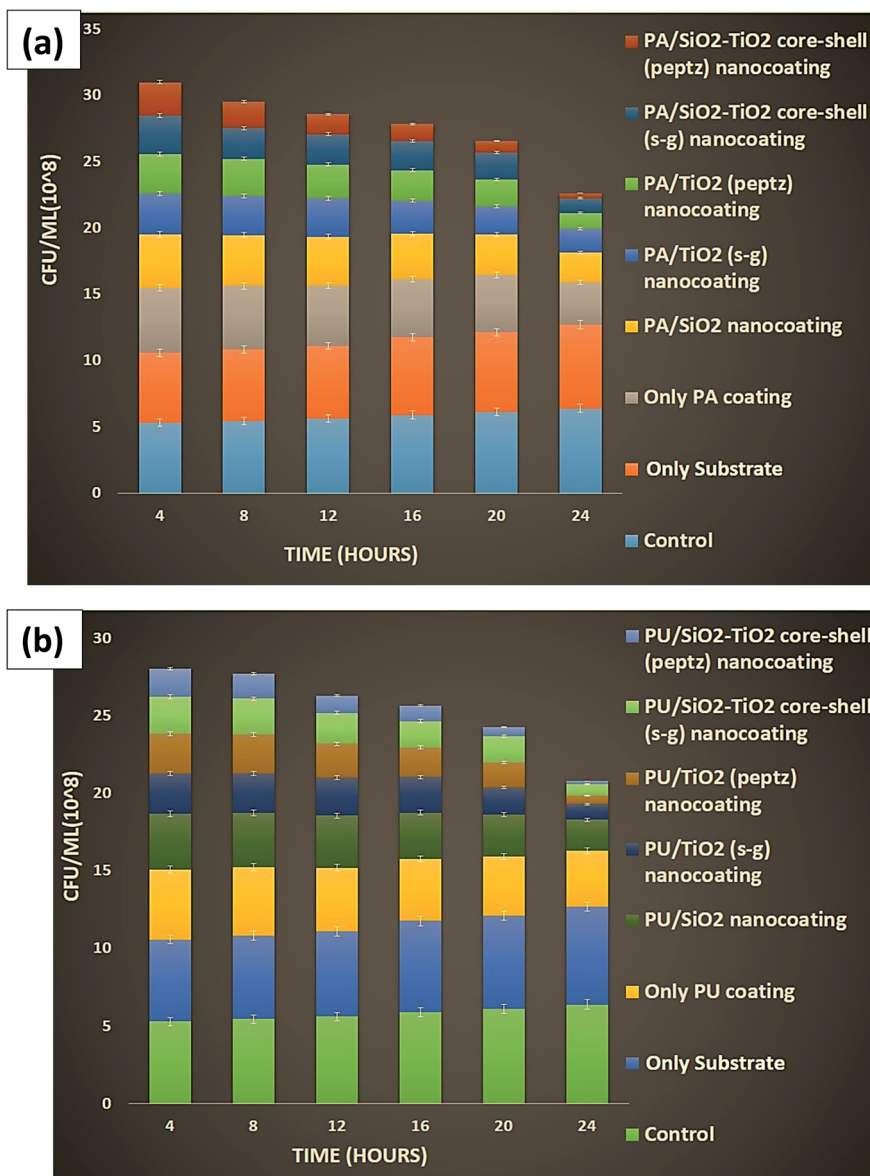
Fig. 11 (a) CFU for poly-acrylic and (b) polyurethane coated substrate (mild steel) containing all prepared nanoparticles against *E. coli*.

Table 5 Optical density data of bacterial culture media containing PA-based nanocoatings with *Bacillus* at 24 h

Material (coatings)	Optical density at 600 nm
Control	0.99
Only substrate	0.89
Pure poly-acrylic (PA) coating	0.68
PA/SiO$_2$ nano-coating	0.59
PA/TiO$_2$ (sol–gel) nano-coating	0.35
PA/TiO$_2$ (peptization) nano-coating	0.26
PA/silica–titania core–shell (sol–gel) nano-coating	0.3
PA/silica–titania core–shell (peptization) nano-coating	0.19

binding energies of 530.8 and 532.2 eV are assigned to the O 1s peak. Apart from the emission peaks of titanium (Ti), oxygen (O) and carbon (C), the silicon (Si) peak was also observed at 99.4 but the count was very low, almost negligible. This XPS result with high Ti counts confirms the formation of a titania shell on the core silica, further confirming the core–shell structure.

4.4 Antibacterial testing analysis

Antibacterial testing was performed against Gram-positive (*Bacillus*) and Gram-negative (*E. coli*) bacteria with all prepared nanoparticles and coatings. Tables 1 and 4 show the optical density values of the bacterial culture media containing free nanoparticles at 600 nm for the anti-bacterial activity against *E. coli* (Fig. 8). The number of live cells (CFU) was also counted for the same species, as shown in Fig. 9. Coating formulations were developed with poly-acrylic (PA) and poly-urethane (PU) at different concentrations of nanoparticles from 1% (wt) to 6% (wt) on a mild steel substrate and tested against

Table 6 Optical density data of bacterial culture media containing PU-based nanocoatings with *Bacillus* at 24 h

Material	Optical density at 600 nm
Control	0.99
Only substrate	0.89
Pure polyurethane (PU) coating	0.62
PU/SiO$_2$ nano-coating	0.59
PU/TiO$_2$ (sol–gel) nano-coating	0.21
PU/TiO$_2$ (peptization) nano-coating	0.15
PU/silica–titania core–shell (sol–gel) nano-coating	0.19
PU/silica–titania core–shell (peptization) nano-coating	0.1

the same bacterial species. We observed that the optimum concentration was obtained at 4% (wt) nanoparticles for both the coatings against *E. coli*. Exceeding the concentration beyond 4% (wt) did not show much improvement. Optical density was checked at 600 nm for all the coated samples at 6 h intervals upto 24 h. Tables 2 and 3 show the final optical density value at 24 h for all the poly-acrylic and polyurethane-based coatings developed with 4% (wt) concentration of nanoparticles against *E. coli* (Fig. 10 and 11).

Tables 5 and 6 show the final optical density value at 24 h for all the poly-acrylic and polyurethane-based coatings developed with 4% (wt) concentration of nanoparticles against *Bacillus* because only 4% (wt) concentration of nanoparticles has shown best results as compared to other concentration in coatings in both of the strains.

The maximum anti-bacterial property was obtained for polyurethane-based nano-coating developed with silica–titania core–shell nanoparticles at 4% (wt) concentration of nanoparticles prepared *via* the peptization process against *Bacillus*. This concentration of nanoparticles completely killed the bacteria within 24 h (Fig. 12–14).

The quantitative examination of *Bacillus* (CFU mL^{-1}) was also performed for all the samples and the best results were found with a coating developed in PU at 4% (wt) concentration of silica–titania core–shell nanoparticles.

CFU mL^{-1} was calculated by using this formula:

$$CFU = \frac{No.\ of\ colonies \times dilution\ factor}{Volume\ of\ the\ culture\ plate}$$

The mechanism behind the growth reduction is that metal oxides carry positive charges and the microorganisms carry negative charges, which cause an attraction between microorganism and metal oxide that leads to the oxidation and finally death of the microorganisms. Nanoparticles also deactivate the cellular enzymes and DNA by coordinating to electron-donating groups such as thiols, carbohydrates, amides, and hydroxyls. This causes cell death.

4.6 Analysis of the mechanical properties of the coating: scratch hardness, adhesion, impact resistance and flexibility

In the Erichsen scratch tester, anti-scratch testing was also performed on mild steel substrate for a 20 N load and found that this mild substrate coating allowed to pass the load up to 20 N successfully. A detailed analysis was carried out *via* scanning electron microscopy. From Fig. 15, it can be seen that only polyurethane coating on mild steel could not bear the load after 5 N but silica-polyurethane coating passed and the silica–titania core–shell nanoparticle/PU-coating easily crossed the load up to 9 N. Therefore, further we tested its mechanical behavior at the industry level. Even at the industrial level, this core–shell/PU coating has shown good anti-scratch performance up to 20 N load at 44% (wt) concentration of nanoparticles in the formulation. It means that silica improved the strength of the PU coating strongly.

The adhesion test was performed for the polyurethane-based coatings and completely satisfactory results were obtained using a cross-hatch test at 1×1 mm, passed (100/100).

These coatings allowed the highest impact resistance of up to 500 grams weight and 50 cm height.
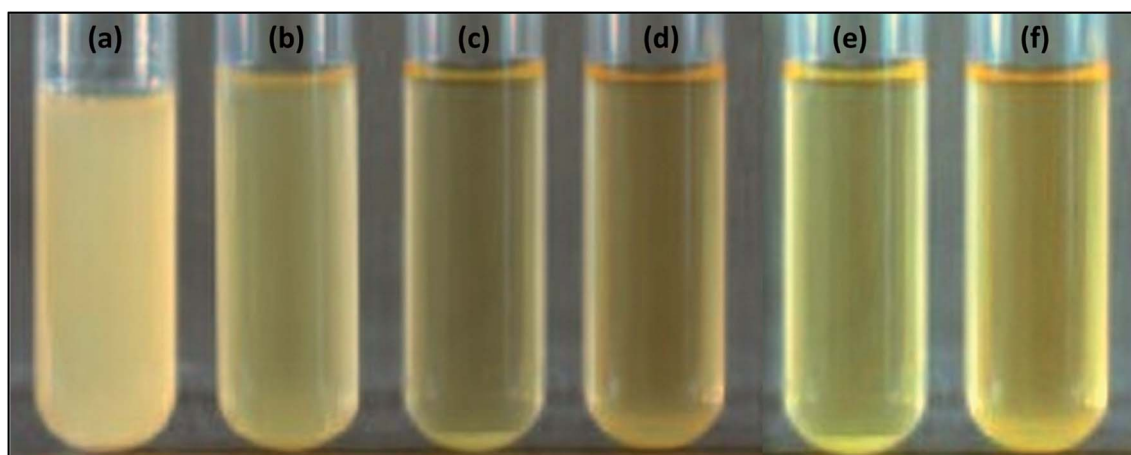

Fig. 12 Anti-bacterial testing of nanoparticles against *Bacillus* (a) control (b) silica nanoparticles (c) titania nanoparticles prepared through the peptization process (d) silica–titania core–shell nanoparticles prepared through the peptization process (e) titania nanoparticles prepared through the sol–gel process (f) silica–titania core–shell nanoparticles prepared through the sol–gel process.
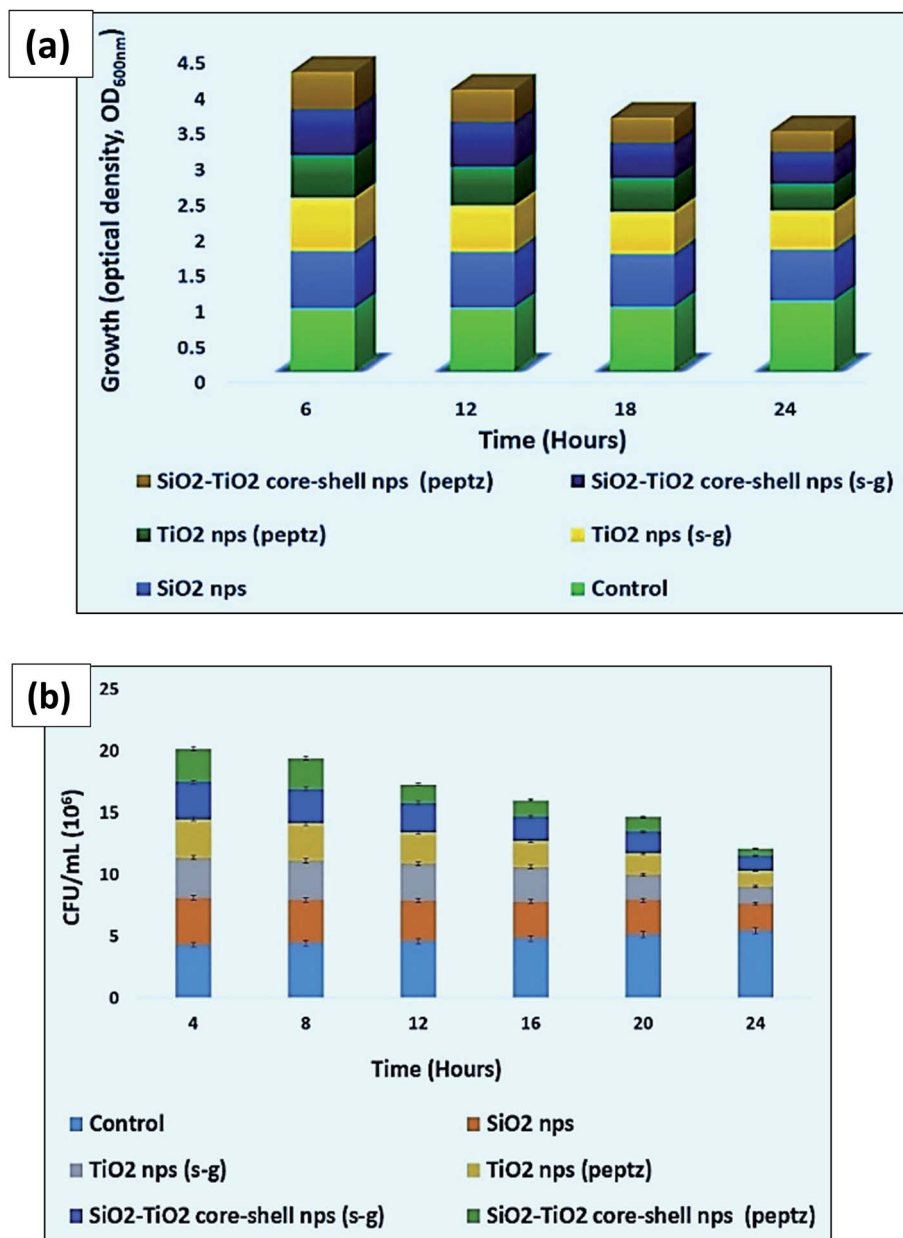
Fig. 13   (a) Optical density and (b) CFU for all prepared nanoparticles in antibacterial testing against *Bacillus*.

The flexibility of these coatings allowed it to pass 12 mm cylindrical mandrel (Table 7).

4.7   Anti-corrosion performance of the coating

An anti-corrosion study was successfully carried out by high humidity testing with no signs of rust or staining at the surface after testing. This test is universal to all types of stainless materials. Humidity can have a significant impact on the performance of the materials and coatings. With humidity testing, the data obtained can be utilized in developing and selection of paints, coatings, paints and materials. By adequately protecting against humidity, the product's lifespan can be extended.

Including all properties mentioned in this article, this coated surface has shown hydrophobic nature also, which was evaluated by a contact angle measurement, *i.e.*, 133.3°. The contact angle data of this surface was already reported in one of our previously published research articles (ref. 33).

The applications of these core–shell based multifunctional nanocoatings can include interior and exterior house paints, interior furnishings, glass and façade coatings for high-rise buildings, all types of transportation vehicles and structures (automobiles, airplanes, bridges, road markings, marine vessels, space-crafts, *etc.* that protect the substrate from a wide range of abuses, *e.g.* damage due to scratches or impact, corrosion, long term weathering and bio-fouling) and a wide variety of industrial and non-industrial maintenance coatings.
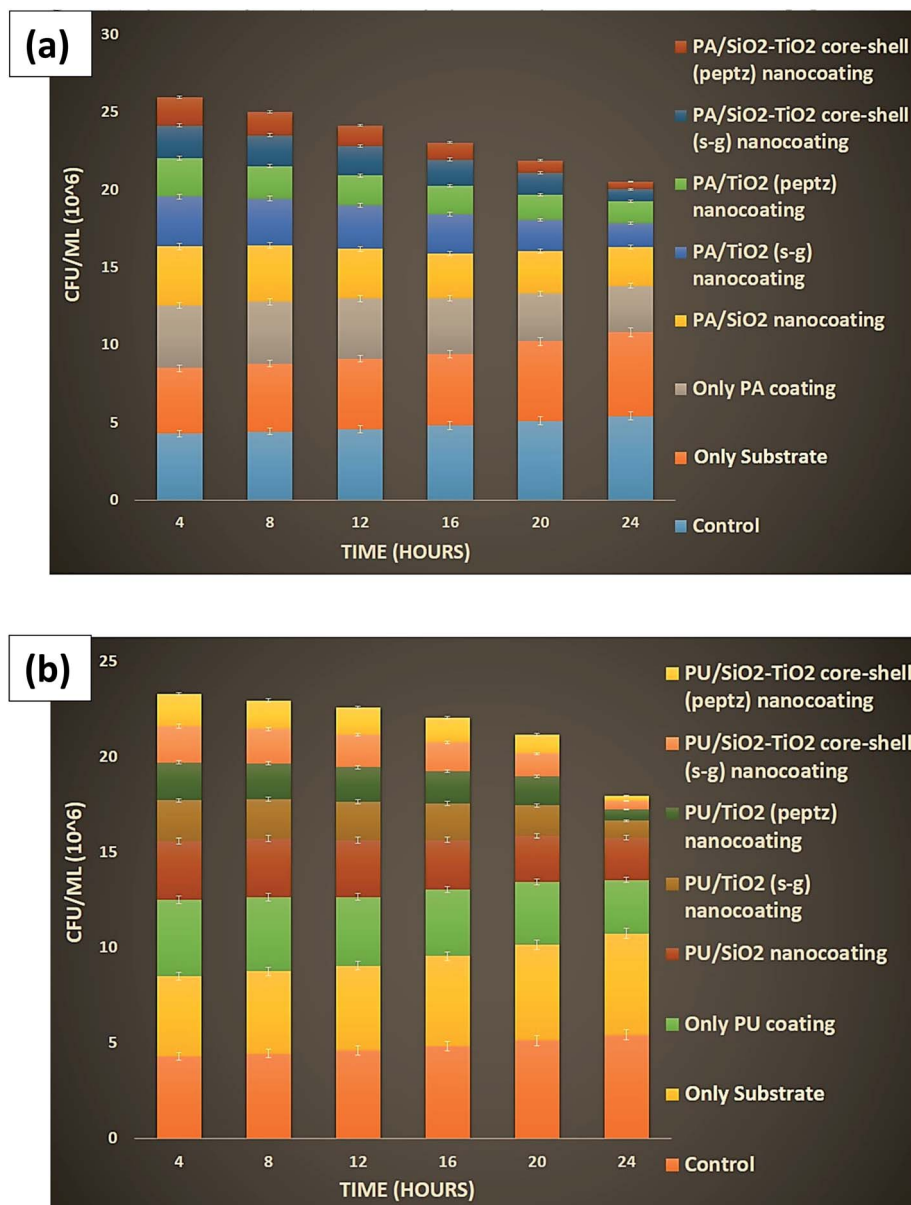
Fig. 14 (a) CFU for poly-acrylic and (b) polyurethane-coated substrate (mild steel) containing all prepared nanoparticles against *Bacillus*.

At a much smaller scale, these coatings can be useful in numerous electronic products (both consumer and industrial electronics) and biomedical products.

5. Conclusion

We successfully prepared super protective coatings using silica–titania core–shell nanoparticles, which are highly antibacterial as well as mechanically-strengthened coatings. To achieve this development, PU and PA-based coating formulations were successfully developed with silica–titania core–shell nanoparticles *via* both sol–gel and peptization processes. Separate paint formulations were also developed with nano-silica and nano-titania individually at the same concentration to compare the antibacterial activity of the core–shell nanoparticle-based

paint with those of paint containing pure silica and pure titania nanoparticles. The antibacterial property against bacteria (*E. coli* and *Bacillus*) were found the best at 4% (wt) core–shell nanoparticles (prepared through a peptization process) based paint formulations in both the binder system-polyurethane and poly-acrylic.

Polyurethane-based coating formulations with silica–titania core–shell nanoparticles prepared *via* the peptization process was used for anti-scratch testing because this preparation method gave the best antimicrobial results. Scratch testing was performed successfully using the Erichsen scratch tester, the formulated PU coating passed up-to 20 N load with good adhesion, impact resistance flexibility and also this coating has shown good anti-corrosion performance.
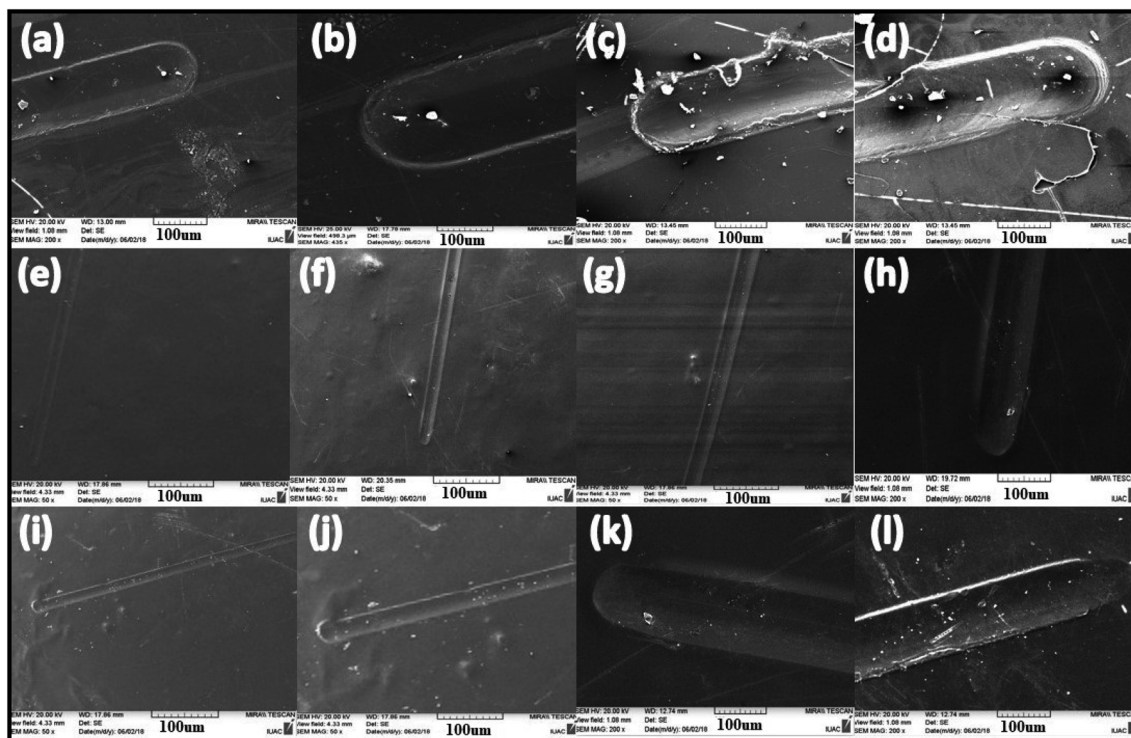
Fig. 15 SEM images at different loads on mild steel (i) scratched polyurethane coating (a) 3 N (b) 5 N (c) 7 N (d) 9 N (ii) scratched polyurethane coating containing silica nanoparticles (e) 3 N (f) 5 N (g) 7 N (h) 9 N (iii) scratched polyurethane coating with silica−titania core−shell nanoparticles (i) 3 N (j) 5 N (k) 7 N (l) 9 N.

Table 7 Mechanical properties of polyurethane-based coating containing silica−titania core−shell nanoparticles prepared through the peptization process

Substrate	MS panel
Application system	By spray without dilution
Finish on panel	Smooth and glossy
Drying condition	Bake at 100 °C for 15 min and air drying overnight
DFT	30–40μ
Adhesion test	Cross-hatch test (1×1 mm) passed (100/100)
Scratch hardness	Up to 2000 grams
Impact resistance	Passed up to 500 g weight and 50 cm height
Flexibility	Passed 12 mm cylindrical mandrel

Conflicts of interest

There are no conflicts to declare.

Acknowledgements

References

1 D. H. Abdeen, M. E. Hachach, M. Koc and M. A. Atieh, A Review on the Corrosion Behaviour of Nanocoatings on Metallic Substrates, *Materials*, 2019, **12**, 1–42.

2 M. Cloutier, D. Mantovani and F. Rosei, Antibacterial Coatings: Challenges, Perspectives, and Opportunities, *Trends Biotechnol.*, 2015, **33**, 637–652.

3 Y. Tanouchi, A. Pai, H. Park, S. Huang, N. E. Buchler and L. You, Long-term growth data of Escherichia coli at a single-cell level, *Sci. Data*, 2017, **4**, 1–5.

4 M. Banning, Bacteria and the gastrointestinal tract: beneficial and harmful effects, *Br. J. Nurs.*, 2013, **15**, 144–149.

5 D. Zachary, Blount The unexhausted potential of E. coli., *Elife*, 2015, **25**, 1–12.

6 M. B. Azad, T. Konya, H. Maughan, D. S. Guttman, C. J. Field, R. S. Chari, M. R. Sears, A. B. Becker, J. A. Scott and A. L. Kozyrkyi, Gut microbiota of healthy Canadian infants: profiles by mode of delivery and infant diet at 4 months, *Can. Med. Assoc. J.*, 2013, **185**, 385–394.

7 S. M. Amato, M. A. Orman and M. P. Brynildsen, Metabolic control of persister formation in Escherichia coli, *Mol. Cell*, 2013, **50**, 475–487.

8 J. Jang, H. G. Hur, M. J. Sadowsky, M. N. Byappanahalli, T. Yan and S. Ishii, Environmental Escherichia coli: ecology and public health implications—a review, *J. Microcomput. Appl.*, 2017, **123**, 570–581.

9 E. T. Dominguez, P. H. Nguyen, H. K. Hunt and A. Mustapha, Antimicrobial Coatings for Food Contact Surfaces: Legal Framework, Mechanical Properties, and Potential Applications, *Compr. Rev. Food Sci. Food Saf.*, 2019, **18**, 1825–1858.

10 G. Othoum, S. Prigent, A. Derouiche, L. Shi and A. Bokhari, Comparative genomics study reveals Red Sea Bacillus with characteristics associated with potential microbial cell factories (MCFs), *Sci. Rep.*, 2019, **9**, 1–13.

11 M. K. Osman, D. K. Anthony, O. Ahmed and S. Al-M. Khalid, Poultry and beef meat as potential seedbeds for antimicrobial resistant enterotoxigenic Bacillus species: a materializing epidemiological and potential severe health hazard, *Sci. Rep.*, 2018, **8**, 1–15.

12 M. Angel and F. Elena, *Mesoporous Silica Nanoparticle*, Wiley-VCH, 2015, vol. 11, pp. 1526–1532.

13 L. Alexander and M. Natalie, Synthesis and surface functionalization of silica nanoparticles for nanomedicine, *Surf. Sci. Rep.*, 2014, **69**, 132–158.

14 B. Charu and A. Upendra, Mesoporous silica nanoparticles in target drug delivery system, *Int. J. Pharm.*, 2015, **5**, 124–133.

15 A. B. Ismail Rahman and P. Vejayakumaran, Synthesis of Silica Nanoparticles by Sol-Gel: Size-Dependent Properties, Surface Modification, and Applications in Silica-Polymer Nanocomposites, *J. Nanomater.*, 2014, **10**, 132–140.

16 M. I. Saira and R. S. Naseem, Synthesis and characterization of titania nanoparticles by sol-gel technique, *Mater. Today*, 2015, **2**, 5455–5461.

17 M. H. Abdel Rehim and M. A. E. Samahy, Photocatalytic activity and antimicrobial properties of paper sheets modified with TiO_2/sodium alginate nanocomposites, *Carbohydr. Polym.*, 2016, **4**, 194–199.

18 C. Euvananont, K. Junin, P. Inpor, P. Limthongkul and C. Thanahayanont, Synthesis, characterization and application of TiO_2 nanopowders, *Appl. Nanosci.*, 2014, **4**, 305–313.

19 F. Kensei, K. Yasutaka, S. Yuki and Y. Hiromi, Fabrication of Photocatalytic Paper Using TiO_2 Nanoparticles, *Langmuir*, 2017, **33**, 288–295.

20 K. S. Kumar, V. B. Kumar and P. Paik, Recent Advancement in Functional Core-Shell Nanoparticles of Polymers: Synthesis, Physical Properties, and Applications in Medical Biotechnology, *J. Nanoparticles*, 2015, **10**, 659–672.

21 J. W. Lee, S. Kong, S. K. Woo and J. Kim, Preparation and characterization of SiO_2/TiO_2 core-shell particles with controlled shell thickness, *Mater. Chem. Phys.*, 2007, **106**, 39–44.

22 F. Wang, M. Li, L. Yu, F. Sun, Z. Wang, L. Zhang, H. Zeng and X. Xu, Corn-like, recoverable γ-Fe_2O_3@SiO_2@TiO_2 photocatalyst induced by magnetic dipole interactions, *Sci. Rep.*, 2017, **7**, 1–10.

23 K. J. Soo, K. S. Jung, J. E. Gu, Y. H. Hui and S. M. Koo, The Preparation of Titania Nano Crystals and Silica-Titania Core-Shell Particles through Peptization Process, *J. Ceram. Process. Res.*, 2013, **14**, 327–331.

24 S. A. Yang, S. Choi, S. M. Jeon and J. Yu, Silica nanoparticle stability in biological media revisited, *Sci. Rep.*, 2018, **8**, 1–9.

25 K. Sato, K. Ishii, Y. Oaki, K. Nakanishi and H. Imai, Polymer-assisted shapeable synthesis of porous frameworks consisting of silica nanoparticles with mechanical property tuning, *Polym. J.*, 2017, **49**, 825–830.

26 A. Kubacka, M. S. Diez, D. Rojo, R. Bargiela and S. Ciordia, Understanding the antimicrobial mechanism of TiO_2-based nanocomposite films in a pathogenic bacterium, *Sci. Rep.*, 2014, **4**, 1–9.

27 S. P. Krumdieck, R. Boichot, R. Gorthy, J. G. Land and S. Lay, Nanostructured TiO_2 anatase rutile-carbon solid coating with visible light antimicrobial activity, *Sci. Rep.*, 2019, **4**, 1–11.

28 J. Wiener, Multiple antibiotic–resistant Klebsiella and Escherichia coli in nursing homes, *J. Am. Med. Assoc.*, 2009, **281**, 517–523.

29 R. Sharma, M. S. Jafari and S. Sharma, Antimicrobial bio-nanocomposites and their potential applications in food packaging, *Food Contr.*, 2020, **112**, 1–11.

30 X. PanIliana, R. Ramirez, R. Mernaugh and J. Liu, Nano-characterization and bactericidal performance of silver modified titania photocatalyst, *Colloids Surf. B Biointerfaces*, 2010, **77**, 82–89.

31 J. Verma, S. Nigam, S. Sinha and A. Bhattacharya, Development of polyurethane based anti-scratch and anti-algal coating formulation with silica-titania core-shell nanoparticles, *Vacuum*, 2018, **153**, 24–34.

32 J. Verma, S. Nigam, S. Sinha and A. Bhattacharya, Comparative studies on poly-acrylic based anti-algal coating formulation with SiO_2@TiO_2 core-shell nanoparticles, *J. Chem.*, 2018, **30**, 1120–1124.

33 J. Verma, S. Nigam, S. Sinha, B. S. Shikarwar and A. Bhattacharya, Irradiation effect of low energy ion on polyurethane nanocoating containing metal oxide nanoparticles, *Radiat. Eff. Defect Solid*, 2018, **172**, 964–974.